Catal Lett (2009) 130:28–36
DOI 10.1007/s10562-009-9851-z

Morphologic Control of Pt Supported Titanate Nanotubes and Their Photocatalytic Property

Takashi Kubo · Masato Takeuchi · Masaya Matsuoka · Masakazu Anpo · Atsushi Nakahira

Received: 28 December 2008 / Accepted: 1 January 2009 / Published online: 24 February 2009

Abstract Morphologic control of Pt supported titanate nanotubes was attempted by the hydrothermal hot-pressing (HHP) technique in order to improve the handleability as a photocatalyst. The bulk of Pt-nanocrystal supported titanate nanotubes was successfully fabricated without the H_2 reduction process by applying the HHP technique. The bulky Pt-nanocrystal supported titanate nanotubes possessed dense microstructures, significantly sharp distributions of mesopores, and high Brunauer–Emmett–Teller (BET) surface area. Furthermore, the bulky Pt-nanocrystal supported titanate nanotubes showed the photocatalytic degradation activities of 2-propanol aqueous solution under UV-light irradiation.

Keywords Titanate · Nanotube · Pt · Photocatalyst · Mesoporous bulk · Hydrothermal hot-pressing · 2-Propanol

1 Introduction

TiO_2-derived nanotubes, which are synthesized by a hydrothermal process of TiO_2 particles in a concentrated NaOH aqueous solution, are notable nanoscale-materials because of their nanotubular structures, high surface areas, and so on [1–8]. For that reason, several application studies on such as electrochromism [9], bone regeneration [10], proton conduction [11], photoinduced hydrophilicity [12], photocatalysts [13–16], and dye-sensitizing solar batteries [17] have been conducted by many researchers.

We have reported Pt-nanocrystal supported TiO_2-derived nanotubes-powders with high photocatalytic ability [15, 16]. In special, Pt-nanocrystal entrapped TiO_2-derived nanotube was successfully synthesized through the hydrothermal process and a subsequent heat-treatment in H_2 atmosphere of the mixture of TiO_2-derived nanotubes and a Pt salt. The aggregation of Pt particles can be prevented by this successful synthesis of Pt-nanocrystal entrapped TiO_2-derived nanotubes.

In order to make full use of the characteristics of these TiO_2-derived nanotubes as several applications, it is important to prevent the non-uniformed aggregation and to control the arrangement of these nanotubes in terms of size and morphology at larger than micrometer or centimeter size, respectively. In fact, many studies on the molophologic control such as preparations of film form and bulk form for these nanotubes have been attempted vigorously [9, 12, 18–20]. On another front, no study on fabrication of bulky TiO_2-derived nanotubes has been performed since a bulk with high density and nanotubular structures was difficult to be fabricated by the conventional method. For instance, in the case of the bulks solidified with silicate, nanotubular structures are filled with amorphous phase as a binder. Furthermore, the sintered body of TiO_2-derived nanotubes could not be fabricated since they could not keep nanotubular structures at high heat. The application area of TiO_2-derived nanotubes can be expected to expand if the fabrication of these bulks becomes possible. For that reason, a bulk formation technique for TiO_2-derived nanotubes needed to be developed. Recently, we have successfully fabricated bulky TiO_2-derived nanotubes with high density by a hydrothermal hot-pressing (HHP) technique [21]. HHP

T. Kubo (✉) · A. Nakahira
Department of Materials Science, Graduate School of Engineering, Osaka Prefecture University, 1-1 Gakuencho, Nakaku, Sakai, Osaka 599-8531, Japan
e-mail: kubo-t@mtr.osakafu-u.ac.jp

M. Takeuchi · M. Matsuoka · M. Anpo
Department of Applied Chemistry, Graduate School of Engineering, Osaka Prefecture University, 1-1 Gakuencho, Nakaku, Sakai, Osaka 599-8531, Japan

is a very useful method for consolidation of ceramic powders at temperatures below 623 K [22]. The compression of samples under hydrothermal conditions enhances the densification of inorganic materials [23–25]. In catalytic applications, it is very important to fabricate the bulk and film form in terms of the handle ability such as a recovery and so on. Moreover, the dense bulk of titanate nanotubes obtained by HHP possessed the mesopores derived from characteristic nano-network structures. Thus, it is speculated that the successful synthesis of bulky Pt-nanocrystal supported TiO_2-derived nanotubes would lead to the expansion of not only applications such as catalysts and dye-sensitizing solar batteries but also new applications.

In the present study, in order to improve the handleability as a photocatalyst, the fabrication of bulky Pt-nanocrystal supported TiO_2-derived nanotubes was attempted by HHP method, and then the structures and photocatalytic properties of obtained bulks were investigated in detail. Photocatalytic properties of samples were evaluated through the degradation of 2-propanol in the liquid phase under UV-light irradiation.

2 Experimental Procedures

2.1 Preparation of Pt Supported TiO_2-Derived Nanotubes Powder

The synthesis of TiO_2-derived nanotubes was attempted via the hydrothermal process. As a source material, commercial anatase-type TiO_2 powder (particle size = 50–100 nm, specific surface area = 3 m^2/g, Kojundo Chem., Osaka, Japan) was used. In this experiment, 2 g of anatase powder was placed inside a Teflon-lined vessel and mixed with 20 mL of 10 M NaOH aqueous solution. The mixture was hydrothermally treated at 383 K 96 h in a stainless bomb. The products were separated by filtration and sufficiently washed with de-ionized water. After a sufficient washing treatment with de-ionized water, obtained powders were dried at temperatures above 323 K in an electric oven for more than 12 h. Then, dried products were mixed with H_2PtCl_6 (Wako Pure Chem. Industries Ltd, Osaka, Japan, 1 wt% of dried products from the hydrothermal treatment) in absolute ethanol. The mixture was stirred for 2 h, evaporated, and dried at temperatures above 323 K in electric oven for more than 12 h. Obtained TiO_2-derived nanotubes with a Pt salt were heat-treated at 573 K for 2 h in air or H_2.

2.2 Fabrication of Bulky Pt Supported TiO_2-Derived Nanotubes

The fabrication of bulky Pt supported TiO_2-derived nanotubes was attempted by HHP method. An autoclave for HHP method used in this study is shown in Fig. 1. The autoclave has a cylindrical body (20 mm in diameter) made of SUS 316, a pair of push rods, teflon grand packings and pistons. Steam pressure in autoclave was kept since teflon grand packings between pistons and rods were transformed by pressing uniaxially. The pistons made water squeezed from the sample powder to escape, and this regulates the appropriate hydrothermal conditions in the powdered sample. Synthesized TiO_2-derived nanotubes-powder with a Pt salt (1 g) was placed in this autoclave for HHP, and deionized water (0.2 mL) was poured into the autoclave. Samples were heated at the rate of 10 K/min under the pressure with 40 MPa, and held at 423 K for 2 h. Obtained bulks were heat-treated at 573 K for 2 h in air or H_2.

2.3 Characterizations

Crystalline phase of samples was determined by X-ray diffraction method (XRD, RINT 2100, Rigaku, Tokyo, Japan) using CuKα radiation at 40 kV and 20 mA. The XRD profiles were collected between 5° and 60° of 2θ angles. Various microstructural analyses were carried out by using a scanning electron microscopy (SEM, S-4500, Hitachi, Tokyo, Japan) with accelerating voltage of 15 kV and a transmission electron microscopy (TEM, JEM2010/SP, JEOL, Tokyo, Japan) with accelerating voltage of 200 kV. Nitrogen adsorption isotherms at 77 K were obtained by automatic gas adsorption measurement apparatus (BELSORP 18PLUS-SPL, Japan-BEL, Osaka, Japan). Some pieces of product were pretreated at 403 K for 10 h.

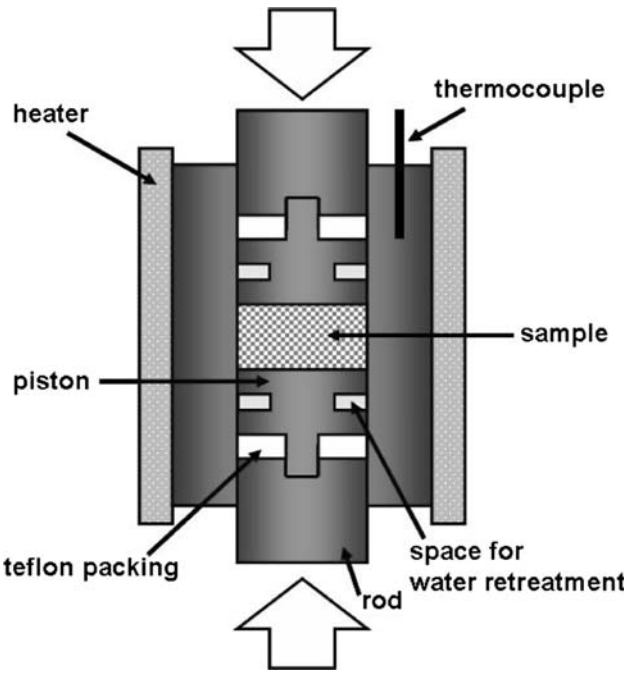

Fig. 1 Autoclave for the hydrothermal hot-pressing used in this study

Bulk density of obtained products was measured by measuring volume and weight.

Pt L_3-edge X-ray absorption near edge structure (XANES) was recorded at room temperature at BL01B1 in SPring-8, Japan synchrotron radiation facility. The operating conditions in the storage ring were at energies of 8 GeV and intensities of about 100 mV. Pt L_3-edge XANES data for the study was collected by fluorescence mode using the two-crystal Si (111) monochromator. The XANES spectra were obtained by subtracting a linear background computed by least-square fitting from the pre-edge region and normalized.

Photocatalytic properties of samples were evaluated through the degradation of 2-propanol. The catalyst (50 mg) was transferred to a glass cell with as aqueous solution of 2-propanol (3.3×10^{-3} M, 25 mL). Prior to UV-light irradiation, the suspension was stirred in a flow of O_2 for 0.5 h at room temperature. The sample was then irradiated at room temperature using UV-light from a 100 W mercury lamp with continuous stirring for 4 h. The products were analyzed by a gas chromatography (GC-14, Shimadzu, Kyoto, Japan) using a flame ionization detector (FID).

3 Results and Discussion

The product prepared by a hydrothermal process possessed nanotubular structures with about 10 nm in outer diameter and 5 nm in inner diameter and a few hundred nm in length, and they were open-end with several wall layers on both sides (not shown in Figure) [5–8, 15, 16, 21]. The XRD pattern of the synthesized nanotubular product in this study was consistent with TiO_2-derived nanotubes prepared in other previous reports. From X-ray absorption fine structure (XAFS) analysis, it was found that these TiO_2-derived nanotubes prepared by the hydrothermal process were mainly composed of titanate compound and that the anatase-like structure was locally present in the titanate based nanotubes [8].

Figure 2 shows XRD patterns of titanate nanotubes and Pt/titanate nanotubes after heat treatments at 573 K in air and H_2 XRD patterns of Pt/titanate nanotubes after heat-treatments were similar with ones of titanate nanotubes without addition of a Pt salt. Figure 3 shows TEM results of Pt/titanate nanotubes after a heat-treatment at 573 K in H_2. TEM and the electron diffraction (ED) results showed that Pt nanocrystals (a few nm in diameter and 5–10 nm in length) with good crystallinity were supported inside these nanotubular titanates with average inner diameter of approximately 5 nm and outer diameter of ~10–15 nm (Figs. 3a–c). Pt-nanoparticles also were in part precipitated on the surface of titanate nanotubes. These Pt-nanoparticles

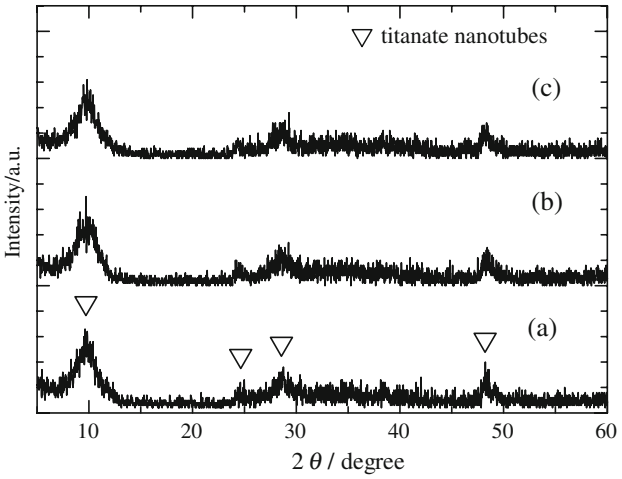

Fig. 2 XRD patterns of (*a*) titanate nanotubes; (*b*) Pt/titanate nanotubes after a heat-treatment at 573 K in air, and (*c*) Pt/titanate nanotubes after a heat-treatment at 573 K in H_2

on the surface of nanotubes were high-dispersive and (111) plane of Pt metal were closely connected with titanate nanotubes (Fig. 3d).

The state of Pt species in titanate nanotubes was also investigated from information on local structure around Pt by Pt L_3-edge XANES measurements. Figure 4a shows Pt L_3-edge XANES spectra of Pt/titanate nanotube before and after heat-treatments at 573 K in air and H_2. XANES for Pt foil and PtO_2 were measured as a reference sample. Figure 4b shows the first derivative regions of Pt L_3-edge XANES spectra shown in Fig. 4a. The edge energy is defined as the energy position corresponding to the peak maximum of the first derivative function. The XANES spectrum of Pt foil revealed lower energy position for the peak maximum of the first derivative function (edge energy), compared with PtO_2. As shown in Fig. 4b, the peak position of the sample after a heat-treatment in air was close to the peak position of PtO_2. On the other hand, the sample after a heat-treatment in H_2 was very close to the peak position of Pt foil, which means that the state of Pt species in the sample after a heat-treatment in H_2 was similar to that of Pt foil. These TEM and XANES results showed the powder of Pt-nanocrystal supported titanate nanotubes was successfully synthesized by the hydrothermal process and a subsequent heat-treatment at 573 K in H_2 (H_2 reduction) of the mixture of titanate nanotubes and H_2PtCl_6.

Photocatalytic properties of these powdered samples were evaluated through the photodegradation of 2-propanol aqueous solution under UV-light irradiation. Under UV-light irradiation, 2-propanol is degraded to form acetone, and acetone as immediate is further oxidized into carbon dioxide and water [26–28]. Figure 5 shows changes in the concentration rates of 2-propanol and acetone with time for

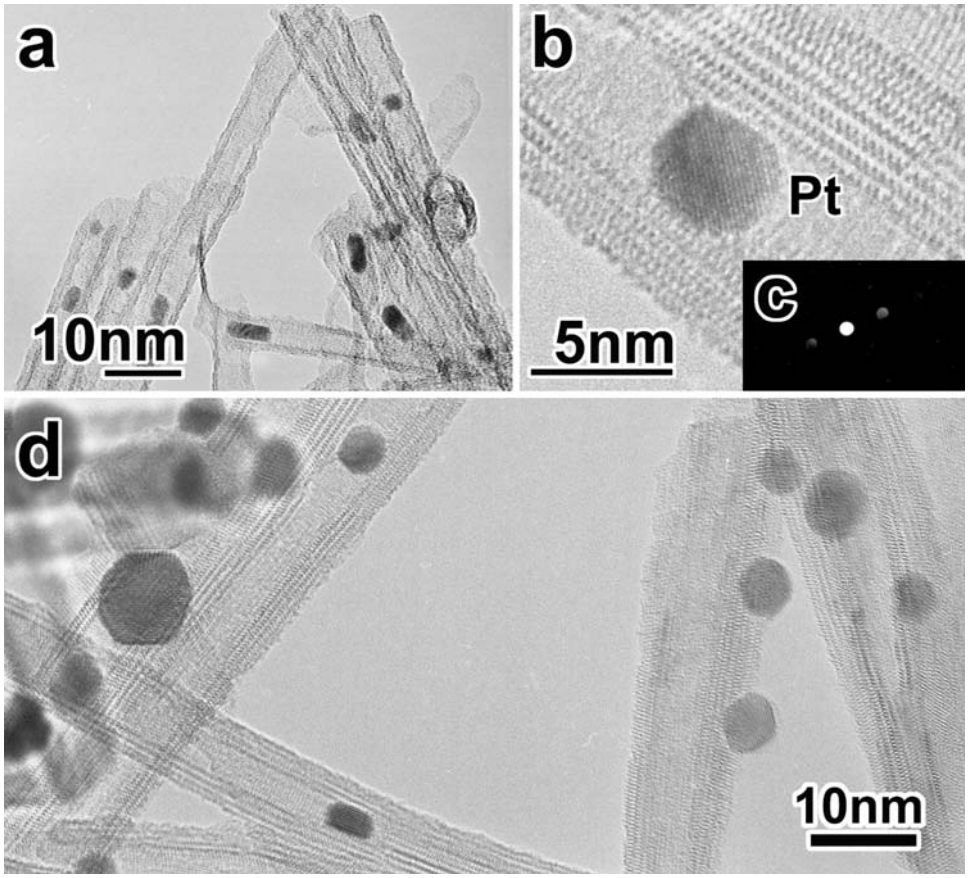

Fig. 3 TEM images of Pt/titanate nanotubes after a heat-treatment at 573 K in H_2. **a**, **d** Low magnification TEM for this sample, **b** enlarged image of; **a**, **c** electron diffraction pattern of **b**, **a** and **d** show different areas

titanate nanotubes-powder, Pt/titanate nanotubes-powders after heat-treatments at 573 K in air and H_2. In the case of using powdered titanate nanotubes and Pt/titanate nanotubes after a heat-treatment at 573 K in air as a catalyst, acetone was not detected though the concentration of 2-propanol aqueous solution showed a decrease of ca. 8% after UV-light irradiation for 4 h (Figs. 5a, b), which means that this decrease of 2-propanol concentration was caused by not the photodegradation but adsorption onto these samples. In contrast, in the case of the powder of Pt/titanate nanotubes after a heat-treatment at 573 K in H_2, acetone generated with a decrease in the concentration of 2-propanol. After UV-light irradiation for 4 h, the concentration of 2-propanol showed a decrease of ca. 11% and the formation ratio of acetone was ca. 7% (Fig. 5c), indicating that this decrease of 2-propanol concentration was caused by not only adsorption onto these samples but also the photodegradation. From results of photodegradation of 2-propanol aqueous solution, it was considered that Pt nanocrystals played a significant role under the present condition and the state of Pt species in titanate nanotubes had much effect on the photocatalytic reaction.

The fabrication of bulky Pt supported titanate nanotubes was attempted by the HHP treatment of titanate nanotubes with a Pt salt and subsequent heat-treatments at 573 K in air or H_2. Figure 6 shows the outside appearance of the bulk prepared by the HHP treatment of titanate nanotubes with a Pt salt under 40 MPa at 423 K for 2 h and a subsequent heat-treatment at 573 K in H_2. The bulk sample prepared by the HHP treatment of titanate nanotubes with a Pt salt under 40 MPa at 423 K for 2 h had the high value of the bulk density of 1.76 g/cm^3, and bulks after heat-treatments in air and H_2 also had the high value of 1.60 and 1.61 g/cm^3, respectively. Figure 7 shows typical SEM images at low and high magnifications for bulks before and after heat-treatments at 573 K in air and H_2. From SEM observations, there were no voids in these bulks (Figs. 7a–c). Therefore, it was found that these Pt-bulks sufficiently kept having the dense microstructures. Figure 8 shows XRD patterns of bulks before and after heat-treatments at 573 K in air and H_2. XRD patterns of these bulks represented almost the same diffraction pattern as that of powdered titanate nanotubes. From SEM observations at high magnification, as shown in Fig. 7, it was found that these bulk samples had nanowhisker like morphologies (Figs. 7d–f). These XRD and SEM results implied that these bulk samples maintained nanotubular structures.

Adsorption/desorption isotherms of these bulk samples were also measured by N_2-adsorption. The BJH method was employed to analyze the pore size distribution. The

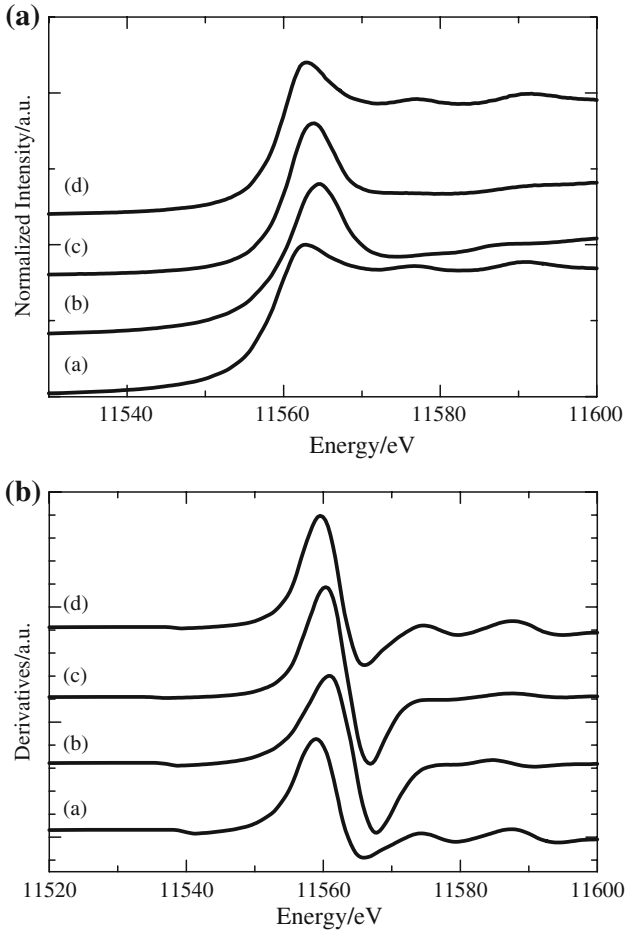

Fig. 4 **a** Pt L_3-edge XANES for (*a*) Pt foil, (*b*) PtO_2, (*c*) Pt/titanate nanotubes after a heat-treatment at 573 K in air, and (*d*) Pt/titanate nanotubes after a heat-treatment at 573 K in H_2; **b** The first derivative functions of Pt L_3-edge XANES spectra shown in **a**

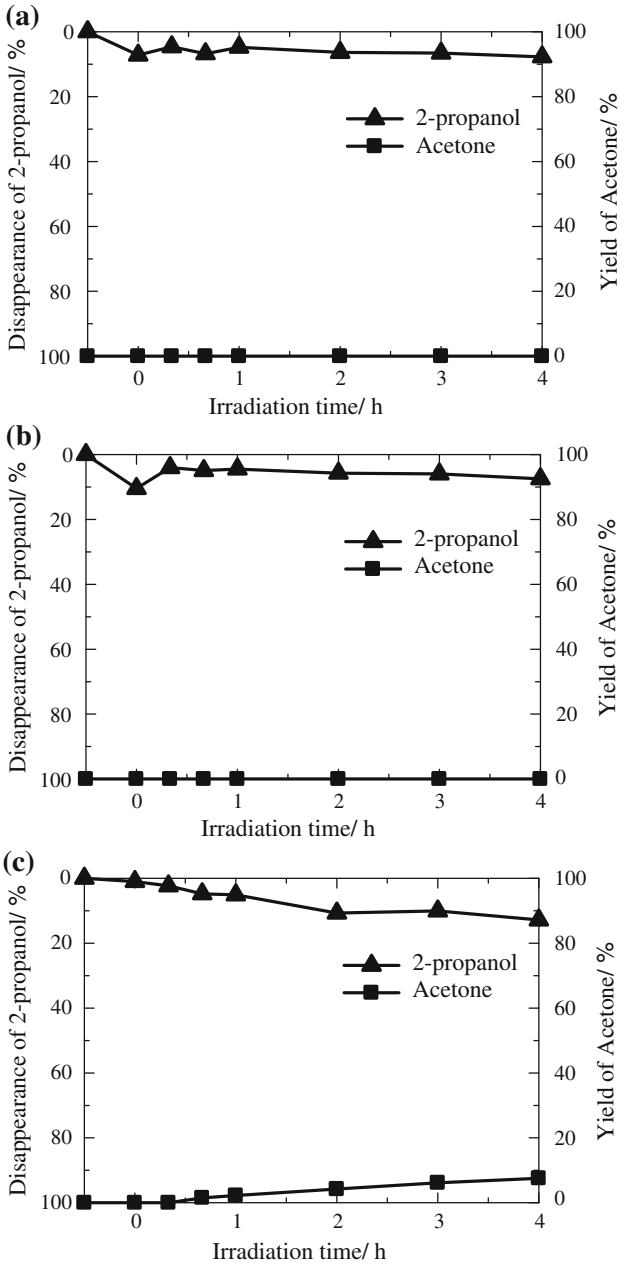

Fig. 5 Reaction time profiles for the liquid phase photocatalytic oxidative degradation of 2-propanol aqueous solution to form acetone on **a** titanate nanotubes; **b** Pt/titanate nanotubes after a heat-treatment at 573 K in air, and **c** Pt/titanate nanotubes after a heat-treatment at 573 K in H_2

typical isotherms and pore size distributions for bulk samples before and after heat-treatments at 573 K in air and H_2 were shown in Fig. 9, respectively. Values of the pore volume, average diameter of pore-size, and BET surface area obtained from N_2-adsorption measurements for these bulks were also summarized in Table 1. As shown in Fig. 9, the adsorption hysteresis for all bulk samples were observed in the region of a relative pressure P/P_0 above 0.4, and the isotherm also represented type IV, suggesting that these bulks possessed mesopores. These bulks also had significantly sharp distributions of mesopores, and the average pore size diameters were ca. 4 nm. Furthermore, these bulks possessed high BET values over 30 m^2/g as listed in Table 1. Here, heat-treatments resulted in a decrease of BET surface area values. The decrease of BET values were derived from not the crystallization of a Pt salt but the breakup of nanotubular structures. In fact, it was obvious that the bulk sample after a heat-treatment in H_2 at 573 K still possessed nanotubular structures according to TEM observations as shown in Fig. 10. Therefore, the crystallization of a Pt salt resulted in a reduction of mesopores existing between nanotubes for the bulk. The state of Pt species in the bulk was also investigated from information on local structure around Pt by Pt L_3-edge XANES measurements.

Figure 11 shows Pt L_3-edge XANES spectra and their first derivative regions of bulk samples before and after

Fig. 6 Outside appearance of the bulk prepared by the HHP treatment of titanate nanotubes with a Pt salt under 40 MPa at 423 K for 2 h and a subsequent heat-treatment at 573 K in H_2

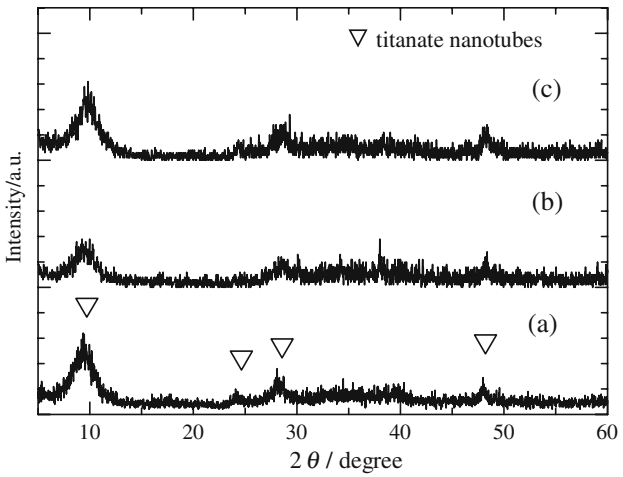

Fig. 8 XRD patterns of (*a*) the bulk prepared by the HHP treatment of titanate nanotubes with a Pt salt under 40 MPa at 423 K for 2 h, (*b*) the bulk prepared by the HHP treatment of titanate nanotubes with a Pt salt under 40 MPa at 423 K for 2 h and a subsequent heat-treatment at 573 K in air, and (*c*) the bulk prepared by the HHP treatment of titanate nanotubes with a Pt salt under 40 MPa at 423 K for 2 h and a subsequent heat-treatment at 573 K in H_2

heat-treatments at 573 K in air and H_2. As shown in Fig. 11b, the peak position of the bulk after a heat-treatment in air was close to the peak position of PtO_2. On the other hand, the bulk after a heat-treatment in H_2 was very close to the peak position of Pt foil, which means that the state of Pt species in the bulk after the heat-treatment in H_2 was similar to that of Pt foil. Thus, in this study, Pt-nanocrystal supported dense mesoporous bulks composed of titanate nanotubes were successfully synthesized. Notably, the bulk of Pt-nanocrystal supported titanate nanotubes was successfully prepared without a heat-treatment process in H_2 atmosphere by applying the HHP technique.

Figure 12 shows changes in the concentration rates of 2-propanol and acetone with time for bulk samples before and after heat-treatments at 573 K in air and H_2. After UV-light irradiation for 4 h, all bulk samples did not collapse

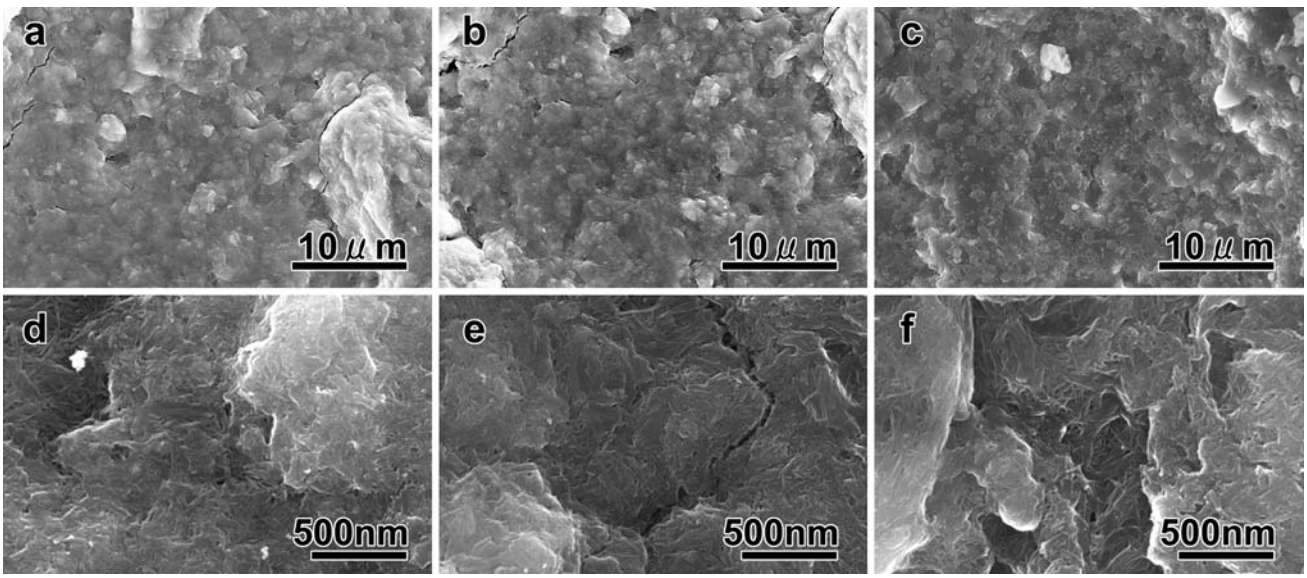

Fig. 7 Typical SEM images of **a**, **d** the bulk prepared by the HHP treatment of titanate nanotubes with a Pt salt under 40 MPa at 423 K for 2 h, **b**, **e** the bulk prepared by the HHP treatment of titanate nanotubes with a Pt salt under 40 MPa at 423 K for 2 h and a subsequent heat-treatment at 573 K in air, and **c**, **f** the bulk prepared by the HHP treatment of titanate nanotubes with a Pt salt under 40 MPa at 423 K for 2 h and a subsequent heat-treatment at 573 K in H_2: Images of **a**, **b**, and **c** were observed at low magnification, and images of **d**, **e**, and **f** were observed at high magnification

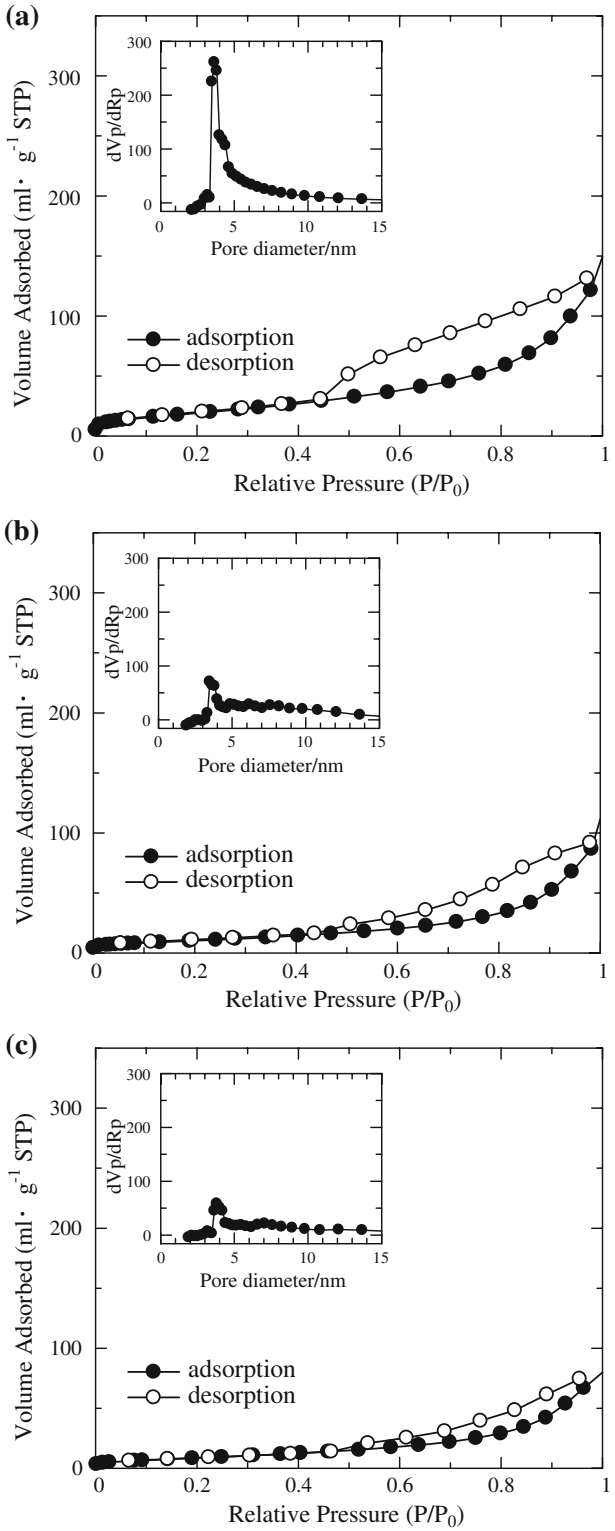

Fig. 9 Typical isotherms and pore size distributions of **a** the bulk prepared by the HHP treatment of titanate nanotubes with a Pt salt under 40 MPa at 423 K for 2 h; **b** the bulk prepared by the HHP treatment of titanate nanotubes with a Pt salt under 40 MPa at 423 K for 2 h and a subsequent heat-treatment at 573 K in air, and **c** the bulk prepared by the HHP treatment of titanate nanotubes with a Pt salt under 40 MPa at 423 K for 2 h and a subsequent heat-treatment at 573 K in H_2

Table 1 Pore diameters, pore volumes, and BET values of the bulk prepared by the HHP treatment of titanate nanotubes with a Pt salt under 40 MPa at 423 K for 2 h, the bulk prepared by the HHP treatment of titanate nanotubes with a Pt salt under 40 MPa at 423 K for 2 h and a subsequent heat-treatment at 573 K in air, and the bulk prepared by the HHP treatment of titanate nanotubes with a Pt salt under 40 MPa at 423 K for 2 h and a subsequent heat-treatment at 573 K in H_2

	Before the heat-treatment	After the heat-treatment in air	After the heat-treatment in H_2
Pore diameter (nm)	3.6	3.7	3.8
Pore volume ($mm^3\ g^{-1}$)	253.0	170.9	134.3
BET value ($m^2\ g^{-1}$)	70.8	37.3	32.6

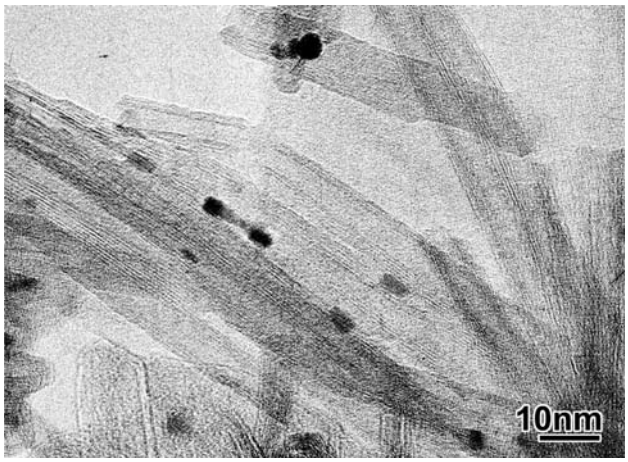

Fig. 10 Typical TEM image of the bulk prepared by the HHP treatment of titanate nanotubes with a Pt salt under 40 MPa at 423 K for 2 h and a subsequent heat-treatment at 573 K in H_2

and keep the bulk shape. In the case of using the Pt/bulk sample after a heat-treatment at 573 K in air, the formation of acetone was not observed though the concentration of 2-propanol decreased with time under UV-light irradiation, which means that this decrease of 2-propanol concentration was mainly caused by the adsorption (Fig. 12b), as in the case of powdered Pt/titanate nanotubes heated in air. On the other hand, in the case of the Pt/bulk sample before and after a heat-treatment at 573 K in H_2, acetone generated with a decrease in the concentration of 2-propanol. After UV-light irradiation for 4 h, the concentration of 2-propanol showed a decrease of ca. 10% and the formation ratio of acetone was ca. 5% (Fig. 12a–c). Thus, these photocatalytic degradation rates were nearly equal to that of the case of Pt-nanocrystal supported titanate nanotubes-powder prepared by H_2 reduction. This result showed that Pt-nanocrystals in the bulky titanate nanotubes were also thought to function adequately for the photodegradation of

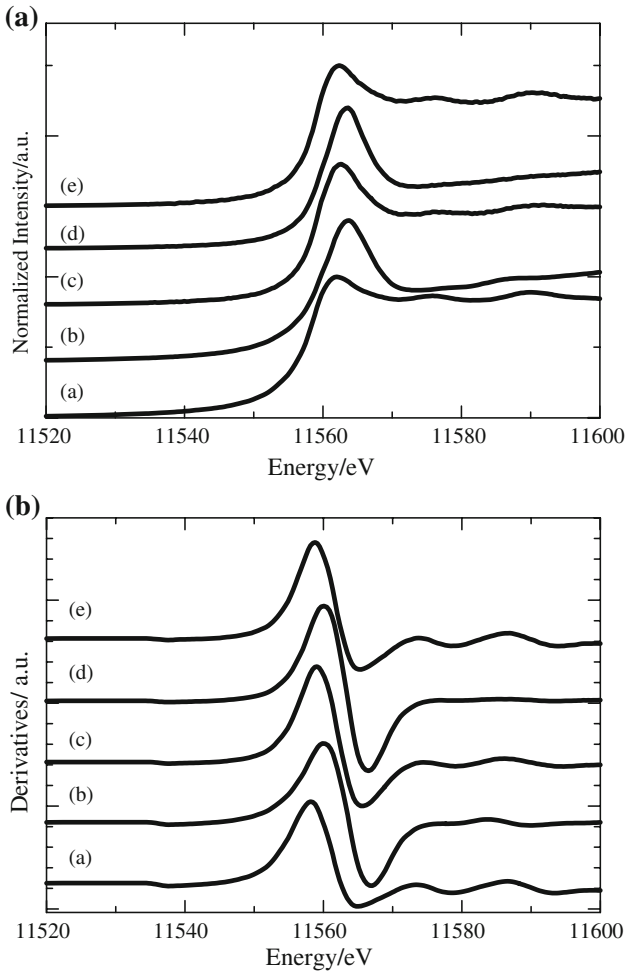

Fig. 11 **a** Pt L_3-edge XANES for (*a*) Pt foil, (*b*) PtO_2, (*c*) the bulk prepared by the HHP treatment of titanate nanotubes with a Pt salt under 40 MPa at 423 K for 2 h, (*d*) the bulk prepared by the HHP treatment of titanate nanotubes with a Pt salt under 40 MPa at 423 K for 2 h and a subsequent heat-treatment at 573 K in air, and (*e*) the bulk prepared by the HHP treatment of titanate nanotubes with a Pt salt under 40 MPa at 423 K for 2 h and a subsequent heat-treatment at 573 K in H_2; **b** The first derivative functions of Pt L_3-edge XANES spectra shown in **a**

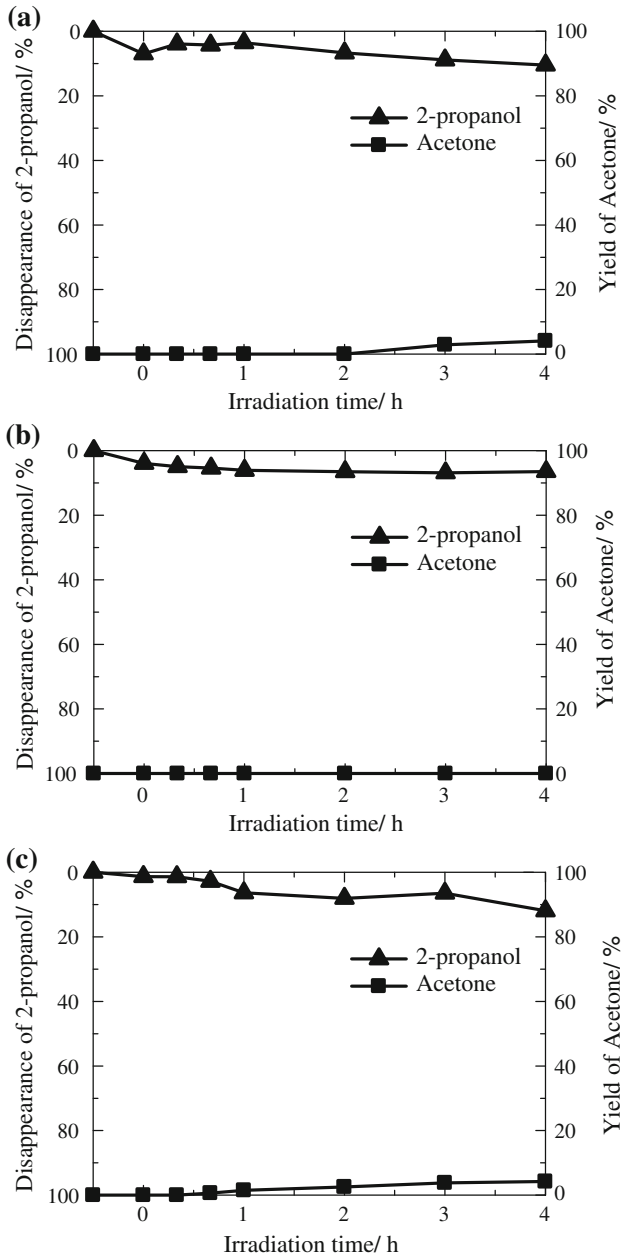

Fig. 12 Reaction time profiles for the liquid phase photocatalytic oxidative degradation of 2-propanol aqueous solution to form acetone on **a** the bulk prepared by the HHP treatment of titanate nanotubes with a Pt salt under 40 MPa at 423 K for 2 h; **b** the bulk prepared by the HHP treatment of titanate nanotubes with a Pt salt nder 40 MPa at 423 K for 2 h and a subsequent heat-treatment at 573 K in air; and **c** the bulk prepared by the HHP treatment of titanate nanotubes with a Pt salt under 40 MPa at 423 K for 2 h and a subsequent heat-treatment at 573 K in H_2

2-propanol aqueous solution. Consequently, the dense bulk with photocatalytic activities of Pt-nanocrystal supported titanate nanotubes was successfully fabricated without the H_2 reduction process by the HHP technique in this study.

4 Conclusions

In this study, titanate nanotubes with about 10 nm outer diameter and 5 nm inner diameter and a few hundred nanometers in length were synthesized by a hydrothermal treatment of anatase-type TiO_2 powder in a 10 M NaOH aqueous solution at 383 K for 96 h. The bulk of Pt-nanocrystal supported titanate nanotubes was attempted fabricated by HHP treatments of titanate nanotubes with a Pt salt and subsequent heat-treatments in air or H_2 in order to improve the handleability as a photocatalyst. The obtained final products were evaluated by various methods such as XRD, SEM, TEM, XAFS, and N_2-adsorption

measurements. Photocatalytic properties of samples were evaluated through the degradation of 2-propanol in liquid phase under UV-light irradiation. The bulks prepared by the HHP treatment and subsequent heat-treatments had dense microstructures, significantly sharp distributions of mesopores, and high BET values over 30 m^2/g. Furthermore, Pt L_3-edge XANES results revealed that the state of Pt species in the Pt/bulk before and after a heat-treatment in H_2 was equal to Pt metal. These bulky Pt-nanocrystal supported titanate nanotubes showed the photocatalytic degradation activities of 2-propanol aqueous solution as well as the powder of Pt-nanocrystal supported titanate nanotubes. Thus, the bulk with photocatalytic activities of Pt-nanocrystal supported titanate nanotubes was successfully fabricated without the H_2 reduction process by the HHP technique. This HHP technique is a useful method to fabricate the functional metal-supported bulk.

Acknowledgments The authors thank Prof. K. Tanaka and Mr. M. Shou of Saitama Institute of Technology for TEM observations. This work was partly supported by the Circle for the promotion of science and Engineering (2008) and Grant-in-aid for Scientific Research from Japan Society for the Promotion of Science (JSPS). XAFS measurements were carried out at BL01B1 in SPring-8 (2007B1666). The authors greatly thank for the technical support and discussion from JASRI.

References

1. Kasuga T, Hiramatsu M, Hoson A, Sekino T, Niihara K (1998) Langmuir 14:3160
2. Chen Q, Du GH, Zhang S, Peng LM (2002) Acta Crystallogr B 58:587
3. Chen Q, Zhou W, Du GH, Peng LM (2002) Adv Mater 14:1208
4. Sun X, Li Y (2003) Chem Eur J 9:2229
5. Nakahira A, Kato W, Tamai M, Isshiki T, Nishio K, Aritani H (2004) J Mater Sci 39:4239
6. Kubo T, Kato W, Yamasaki Y, Nakahira A (2006) Key Eng Mater 317&318:247
7. Kubo T, Yamasaki Y, Nakahira A (2007) J Ion Exchange 18:310
8. Kubo T, Nakahira A (2008) J Phys Chem C 112:1658
9. Tokudome H, Miyauchi M (2005) Angew Chem Int Ed 44:1974
10. Kubota S, Johkura K, Asanuma K, Okouchi Y, Ogiwara N, Sasaki K, Kasuga T (2004) J Mater Sci Mater Med 15:1031
11. Thorne A, Kruth A, Tunstall D, Irvine JTS, Zhou W (2005) J Phys Chem B 109:5439
12. Tokudome H, Miyauchi M (2004) Chem Comm 958
13. Adachi M, Murata Y, Harada M, Yoshikawa S (2000) Chem Lett 29:942
14. Akita T, Okumura M, Tanaka K, Ohkuma K, Kohyama M, Koyanagi T, Date M, Tsubota S, Haruta M (2005) Surf Interface Anal 37:265
15. Nakahira A, Kubo T, Yamasaki Y, Suzuki T, Ikuhara Y (2005) Jpn J Appl Phys 44:690
16. Kubo T, Nagata H, Takeuchi M, Matsuoka M, Anpo M, Nakahira A (2008) Res Chem Intermed 34:339
17. Uchida S, Chiba R, Tomiha M, Masaki N, Shirai M (2002) Electrochemistry 70:418
18. Tian ZR, Voigt JA, Lin J, Mckenzie B, Xu H (2003) J Am Chem Soc 125:12384
19. Liu A, Wei M, Honma I, Zhou H (2005) Anal Chem 77:8068
20. Yada M, Inoue Y, Uota M, Torikai T, Watari T, Noda I, Hotokebuchi T (2007) Lamgmuir 23:2815
21. Kubo T, Yamasaki Y, Nakahira A (2007) J Mater Res 22:1286
22. Yamasaki N, Yanagisawa K, Nishioka M, Kanahara S (1986) J Mater Sci Lett 5:355
23. Nakahira A, Takezoe S, Yamasaki Y (2004) Chem Lett 33:1400
24. Takimura M, Nagata H, Yamasaki Y, Suzuki T, Ikuhara Y (2006) J Ceram Soc Jpn 114:554
25. Nagata H, Takimura M, Yamasaki Y, Nakahira A (2006) Mater Trans 47:2103
26. Yamashita H, Honda M, Harada M, Ichihashi Y, Anpo M, Hirao T, Itoh N, Iwamoto N (1998) J Phys Chem B 102:10707
27. Yamashita H, Nishida Y, Yuan S, Mori K, Narisawa M, Matsumura Y, Ohmichi T, Katayama I (2007) Catal Today 120:163
28. Chavadej S, Phuaphromyod P, Gulari E, Rangsunvigit P, Sreethawong T (2008) Chem Eng J 137:489